TECHNICAL MEMORANDUMS

NATIONAL ADVISORY COMMITTEE FOR AERONAUTICS

No. 825

THE SOURCE OF PROPELLER NOISE

By W. Ernsthausen

Luftfahrtforschung
Vol. XIII, No. 12, December 20, 1936

Washington
May 1937

NATIONAL ADVISORY COMMITTEE FOR AERONAUTICS

TECHNICAL MEMORANDUM NO. 825

THE SOURCE OF PROPELLER NOISE*

By W. Ernsthausen

SUMMARY

Experiments made on a model propeller revealed the following results:

1. The recorded pressure field agrees with the theoretically defined field to within explainable discrepancies.

2. The sound field of a propeller is set up by "radiators," stationary in space, in the immediate proximity of the blades, their radiating depending only on the changes sustained by the field at these points.

3. Two propellers having the same diameter, equal frequency, and the same value of pressure-field change along the radius on either side at equal distance from the plane of the propeller, produce the same noise intensity.

4. Volume and spectrum of the produced sound pressure can be influenced by the form of the blade and the angle of incidence.

5. The higher components are also well represented in the sound spectrum of a normal propeller.

6. Obstacles near the blade amplify the noise and alter the directional effect.

7. The rotation note is radiated preponderatingly in the direction of the plane of the propeller; the rotation noise in the direction of the propeller axis. The spectrum and directional characteristic are influenced by modification of the profile form.

8. For a propeller with low loudness level the resultant tip speed must not exceed 250 meters per second.

---

*"Zur Entstehung des Luftschraubengerausches." Luftfahrtforschung, vol. 13, no. 12, December 20, 1936, pp. 433-440.

9. The order of magnitude of acoustical power in the case considered is about 1 percent of the power loss of the propeller. This value decreases as the tip speed decreases.

I. INTRODUCTION

On the basis of various studies on propeller noise (cf. references), a number of predictions can be made as regards frequency, relation of sound pressure to different operation conditions and propeller constants, and the directional effect of the noise radiated. Save for a few exceptions these reports, however, treat only specific cases. In view of the complex nature of the processes involved, the experiments were made in a simple and comprehensive manner so as to provide basic data.

A two-blade propeller of 40 centimeters diameter and zero pitch was explored for its noise development (figs. 1 and 2); it could be whirled up to 17,000 r.p.m. - i.e., a tip speed of 355 meters per second. It was driven over a 1:5 reduction gear by a 5-kilowatt direct-current motor, whose speed was regulated by a Leonard controller.

To obtain the power loss (N_m) of the propeller for comparison with the produced acoustical power (N_A) the engine performance characteristics were measured with (fig. 2a) and without propeller (fig. 2b). The result is the sought-for relation c, that is, curve c' after correction with the engine efficiency.

To keep the measurements free from the disturbing engine and gear noises, the propeller was acoustically isolated from the drive. Only the propeller and about 0.5 meter of its shaft protruded in a separate room divided from the drive proper by a brick wall and insulated with acoustic plates and a layer of 25-centimeter wide upright cotton-wool sheets (fig. 6).

II. TEST EQUIPMENT

The investigation covered the determination of the pressure distribution in the vicinity of the propeller blades; and the measurement and analysis of the sound pressure.

The pressure field surrounding the propeller blade was ascertained by a pressure indicator so dimensioned as to produce a minimum of field distortion. It consisted of a condenser (system) fitted in a 3.5-centimeter sphere, having a thin aluminum membrane of 12 millimeters diameter, and so arranged as to fair in the outside of the sphere. The pressure indicator is hooked to the first amplifier stage (NF hook-up) by a thin tubing of 0.5 meter length insulated with amber (figs. 3a and 3b).

The frequency curve of the instrument (fig. 4a) can be electrostatically obtained with an auxiliary electrode. Owing to its minimum sound-field distortion, the pressure indicator is equally serviceable as recording microphone. There being no empty space before the membrane, the statically obtained frequency curve with allowance for the sound-pressure rise due to reflection, represents the field calibration (fig. 4b). The directional effect of the microphone is small even for high frequencies.

The correlation of pressure field to blade position was established by optical determination of the blade motion. A pencil of light striking a photoelectric cell is intercepted by the leading edge of the blade when it or the opposite blade faces the center of the membrane of the pressure meter. Thus the blade position relative to the pressure field corresponds to the time interval of the interruption, and the blade width to the duration of the interruption. The currents of the photoelectric cells were jointly recorded with the microphone currents by oscillograph after suitable amplification.

The sound pressure in the room was recorded by a condenser microphone, fitted together with the first amplifier stage in a 15-centimeter spherical housing. The electrostatic frequency curve of this microphone is reproduced in figure 5. The currents for the pressure meter and for the microphone were suitably amplified with constant-frequency transmission. The pressures were so recorded that a variable stepwise compensated calibration line (S. & H.) reproduced a constant deflection on the original instrument.

Certain frequency zones, such as rotation note and rotation noise, for instance, were separated for the study with the octave filter and a variable coil linkage.

As the appraisal of the noise pattern is contingent

upon the knowledge of its composition and directional effect, the spectrum was determined at points of the acoustic field lying on a circular trajectory with the propeller as center. These analyses were made with the Siemens-Halske tone frequency spectrometer.

For recording the directional effect of the propeller the sound-pressure meter was outwardly adjustable by cable and pulley over a quarter circle of 1.25-meter radius about the propeller, which was ample in view of the symmetry of the explored model in the propeller plane (fig. 6).

III. MEASUREMENTS

1. Pressure and Acoustic Field

In reference to the results published heretofore (reference 2), it is logical to assume that the static-pressure field rotating along with the propeller blade is the exciter of the periodic sound field (rotation note). Since the periodic of the blades on the radiating particles causes them to become origins of sound waves, the propeller sound field may be visualized as a circular ring, densely packed by elementary radiating particles which interfere with the rotation phase. Viewed from the acoustic side, there appears in place of the pressure-field distribution in a fixed point in space the time lapse of pressure change of the elementary radiator, whereas sound pressure always refers to the pressure at a point of the sound field set up by the whole propeller. As the increases of speed of the medium particles appearing at the propeller blade themselves return to sound velocity in the immediate vicinity, the relation of sound field to pressure field is then only available from the propagation phenomena. The pressure field forming around a profile moving at uniform speed in a medium has been extensively treated in aerodynamic works on the basis of the theory of plane potential flow.

For an approximate field calculation the profile may be replaced by a double source superposed by a parallel flow (reference 3). The so-computed field of the employed profile in symmetrical flow is illustrated in figure 7. The field distribution along the flow direction is shown in figure 8, for three different distances.

The field pressure is obtained at

$$p_o \approx \lambda \rho \frac{u^2}{x^2} \qquad (1)$$

where u is the profile velocity

x, distance in propeller axis direction

ρ, air density

λ, a value dependent on profile chord d which, at great values of u (approaching sonic velocity c) may be expressed by (reference 3)

$$\lambda \approx d\, e^{\left(\frac{u}{c}\right)^4} \qquad (2)$$

The field increases with u^2 and decreases with $1/x^2$. But as the reading of the pressure meter gives the effective value p of the distribution shown in figure 8 rather than p_o, and as this distribution equally changes roughly linearly with x along the profile axis, we have:

$$p \approx \lambda \rho \frac{u^2}{x} \qquad (3)$$

The effective value of the pressure change rises with u^2 and drops with $1/x$. With a view of ascertaining whether the pressure change recorded by the pressure receiver is attributable to the profile field and not, perhaps, to the field of the vortices, the relative position of the propeller blade is established in the manner described in section II.

Figure 9 is the oscillographic record of the field distribution (fig. 8). The lower curve represents the blade position, the start of the current peaks denoting the position of the leading or the trailing edge. The differences between calculation and test can be explained by the unrealizable hypothesis of the two-dimensional potential flow by the profile form not completely considered in the calculation, and by the small field distortion of the pressure meter as well as by unavoidable defects in the pressure measurements.

The spatial decrease of the pressure field was measured up to 80 millimeters distance. At that distance

there still was no perceptible instrumental disturbance by the field of the opposite blade or the vortex noise according to oscillographic observation. The result is illustrated in figure 10 for $u = 50$ m/s. The effective value of the pressure-field change drops with $1/x$ (equation 3).

The relationship existing between pressure field, acoustic field, and tip speed was established by observation of the sound pressure at 1.25 meters distance, and of the field pressure at 5 centimeters away. The results are given in figure 11. Up to the relatively small tip speed of 140 meters per second, the theoretical field pressure varies with u^2 (equation 1), but the sound pressure at a higher power, so that the latter may be expressed with

$$p' = p\ f\ (u) \tag{4}$$

Even a measurement as high as 280 meters per second tip speed confirms this relationship (fig. 12). At high speeds, of course, the pressure field itself is no longer related as the square with u. The introduction of (2) in (1) extends that relation. The measurements at high pressures are difficult because of the sensitivity of the instruments and they are therefore afflicted with considerable errors.

Since a rise in tip speed is followed by a proportional rise in the fundamental frequency f_1 of the sound pressure ($f_1 = \frac{nz}{60}$; n = r.p.m., z = number of blades), the sound pressure corresponding to the directional characteristic in a point must be connected with the field pressure over a function of the frequency. According to (4) the sound pressure is:

$$p' = p\ J_{(qz)}\left[\frac{q\ z\ \omega\ R}{c}\ \sin\ \vartheta\right] \text{const.} \tag{5}$$

where $J_{(qz)}$ is the Bessel function of the order of qz

q, ordinal number of the harmonics

R, propeller radius

ϑ, angle between propeller axis and starting point of the straight line

u, ω R

The function $f(u) = J_{(qz)}\left[\frac{qzu}{u}\sin\vartheta\right]$ for a point of the directional characteristic (ϑ = const.) depends, as a result, on the propeller dimensions, the speed, and the ordinal number of the particular harmonics; that is, on the spectrum.

Figure 12a shows $\frac{p'}{p} = f(u)$ plotted against u, curve a denoting the experimentally (fig. 12) obtained variation for the total pressure, and the other curves the variation computed for the first, fourth, and eighth harmonics. Owing to the necessary simplifications incidental to the calculation, it must suffice if these variations correspond. The greatest deviation is probably that the real overtone distribution is not in accord with that numerically assumed.

For the comparison with the field change (fig. 9) the sound pressure was oscillographed at 1.25 meters in the propeller plane (fig. 13). The high vortex frequencies disturbing the picture of the periodic pressure distribution were cut off with a coil linkage, leaving a pattern similar to the field distribution.

The conclusion is that the composition of the sound pressure is related to the configuration of the pressure field and consequently, to the shape and width of the profile and the angle of setting. But if this is so, the formation of the periodic pressure noise of the propeller may be visualized as follows: The pressure fields formed around the propeller blades set up in periodic sequence in every point in space a pressure change:

$$-\rho\frac{\partial\varphi}{\partial t} = -\rho u\frac{d\varphi}{ds}$$

(φ = velocity potential of profile field). From these primary pressure disturbances excited at profile velocity u and having the function of radiators, secondary sound waves are propagated at sonic velocity. The magnitude and time rate of change of sound pressure are, however, primarily governed by the radiators existing in blade proximity at the place of maximum field change.

2. Obstacles in the Pressure Field

Since only the periodic change of the field pressure

is audible, the existence of obstructions in the propeller field must result in a field disturbance

$$-\rho \frac{\partial \varphi}{\partial t}$$

dependent on blade speed and consequently a higher sound pressure.

The sound pressure caused by obstructions in blade vicinity was recorded as a function of the distance of the obstacle from the propeller plane at 137 meters per second tip speed, which produces but little pressure noise. Figure 14 illustrates the directional characteristics in the presence of an obstacle covering the entire propeller diameter. Instead of this obstacle, two radiators in-phase may be visualized, having their principal maximum directional characteristic in direction of the axis (fig. 15a), while an obstacle facing only the radius of the propeller disk may be considered as single radiator (fig. 15b) which, because of its small extent compared with the wave length, reveals no substantial directional effect.

Figure 16 shows the sound intensity proportional to the area of the directional characteristic plotted against the distance of the obstacle. The effect of the obstacle in this case is confined to the immediate vicinity of the blade, although larger pressure fields, such as appear at normal tip speeds and with pitched propellers, have a correspondingly greater effective range.

In this connection it might perhaps be added that a nonuniform air stream has, for the same reasons, a similar effect on the propeller as an obstacle.

3. Spectrum

According to the literature (references 2 and 5), the understanding prevails that the fundamental note supplies the biggest share of the propeller noise. This holds true with certain limitations. When the form of the pressure field is decisive for the composition of the sound pressure, then in propeller proximity with the customary profile forms of metal propellers, the higher overtones must equally well be represented. The very substantial effect of the angle of setting on the pressure field was hereby disregarded. Figure 17 gives the sound intensity of the harmonics plotted against the tip speed - results obtained

from directional characteristics determined from sound pressure surveys. The proportion of the fundamental note is insignificant, while the fifth to tenth harmonics predominate. The possibility of influencing the spectrum rests on the alteration of the blade design and the incidence.

4. Directional Effect

The directional effect of the rotation note is theoretically described by equation (5), according to which the principal maximum of the sound pressure occurs in the plane of the propeller. The measurements show the same result. Figure 18 gives the directional effects of the fundamental note for various tip speeds. Higher tip speed - and with it, higher radiator frequency - are followed by secondary maxima.

Figures 19 to 21 give the directional effect for one revolution each of the individual components as obtained by the spectrometer. For low tip speeds (fig. 19) the components above 2,500 Hz (fig. 22) are predominantly vortex noises because of the radiation in axis direction. As the r.p.m. (frequency) increases, these frequencies disappear from the analyzer (fig. 20), whose range is only 5,000 Hz. The secondary maxima at higher frequency are readily observed in figure 21.

The directional effect can be influenced by changes in profile form, propeller diameter (radiator distance), and propeller speed. The rotation noise was so far not treated on account of its lesser importance, especially since in the present case - contrary to practice - the vortex frequencies are high. The characteristics shown in figure 22 are merely for the purpose of comparison with the data from the appended references. The principal maximum is turned through 90° against that of the rotation note; that is, it lies in axis direction. Whether this directional effect is attributable to the radiator effect of a vortex ring whose single radiators are small relative to the wave length and symmetrically arranged with respect to the profile axis, remains to be proved.

5. Tip Speed

In view of the relation of created sound pressure to the change in the pressure field in a point in space, the tip speed of the propeller assumes a marked significance.

Its effect is clearly to be seen in figure 23, where the curves represent the sound intensity determined from directional effects as function of the tip speed, curve a applying to the recorded rotation note, curve b to the comparative rotation note built up from the analyzers, and curve c, the rotation noise. The sound intensity is shown to drop 95 percent as the tip speed drops from 340 to 250 meters per second. Figure 24 gives the ratio of acoustical-power to propeller-power loss in percent versus tip speed.

Translation by J. Vanier,
National Advisory Committee
for Aeronautics.

REFERENCES

1. Freystedt: Z. f. tech. Physik, Bd. 12 (1935).

2. Obata und Mitarb: Rep. Aeron. Res. Inst., Tokyo: (1932), No. 79; (1932), No. 80; (1933), No. 99; (1933), No. 132.

3. Weinig, F.: Luftfahrtforschung Bd. 12 (1935), S. 222.

4. Paris: Phil. Mag., vol. 13 (1932).

5. Kemp, C. F. B.: Proc. Phys. Soc., vol. 44 (1932); vol. 45 (1933).

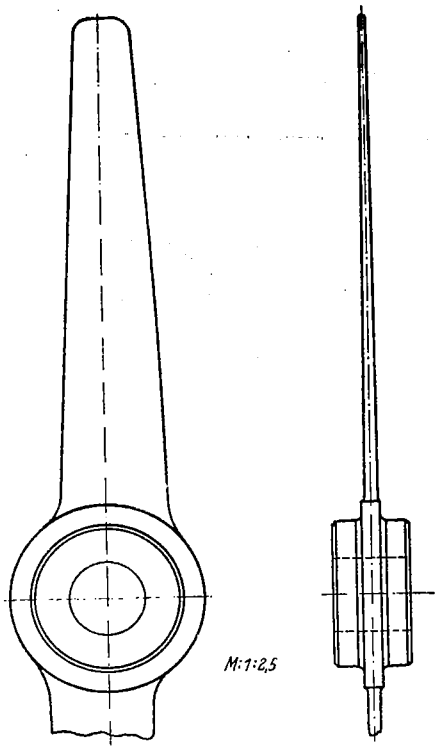

Figure 1.- Model propeller.

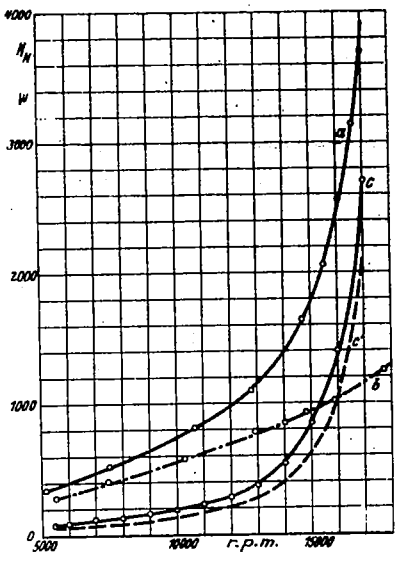

Figure 2.- Power required versus engine and propeller r.p.m.

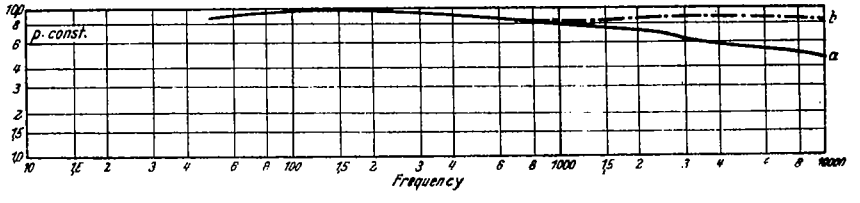

Figure 4.- Frequency curve of pressure meter.

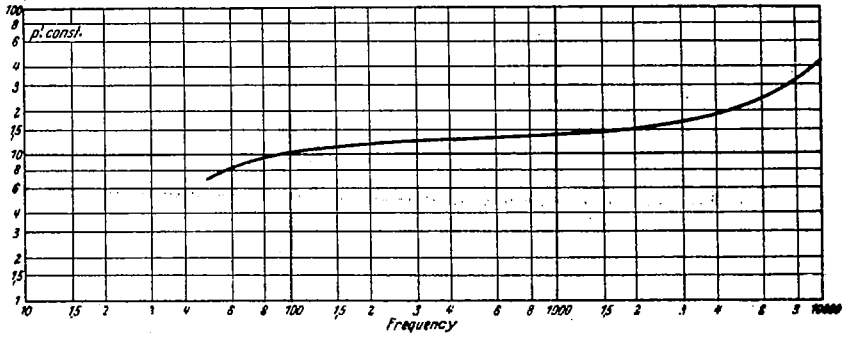

Figure 5.- Frequency curve of microphone.

Figure 3a.- Pressure meter.

Figure 3b.- Pressure meter with first-stage amplifier.

Figure 6.- Experimental arrangement.

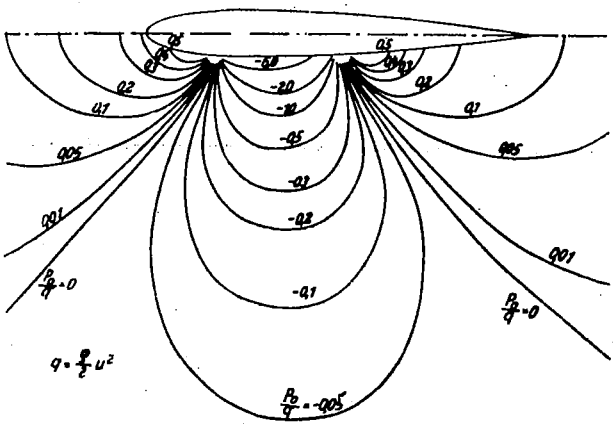

Figure 7.- The computed pressure field of the employed profile.

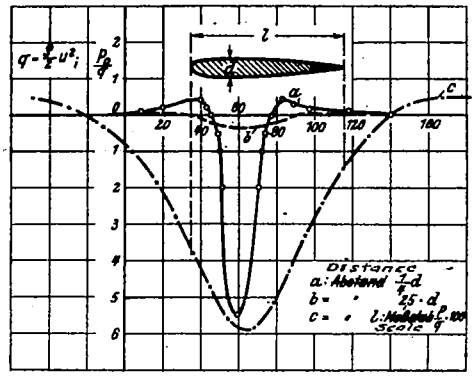

Figure 8.- Computed pressure field distribution along the flow direction.

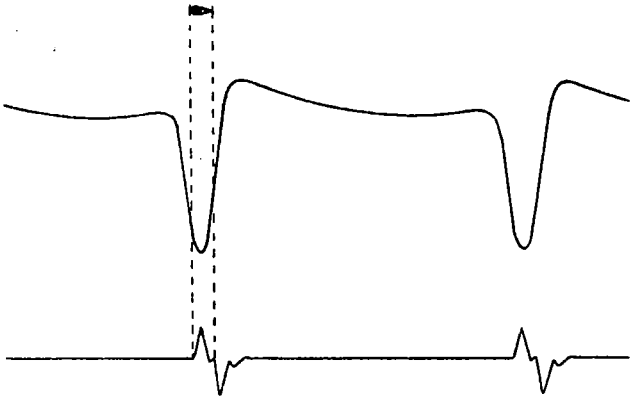

Figure 9.- Oscillogram of pressure field distribution .

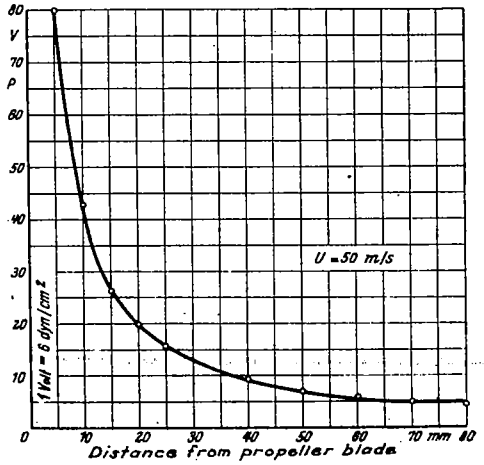

Figure 10.- Effective value of pressure field change versus axial distance from propeller blade.

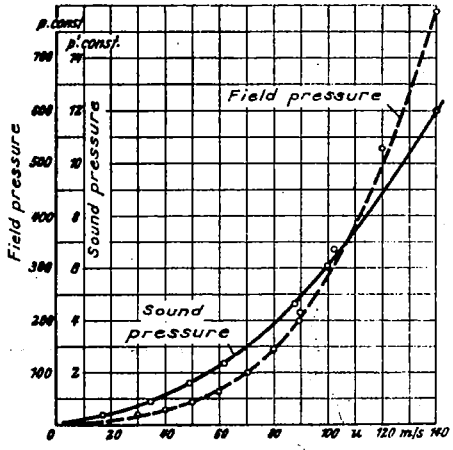

Figure 11.- Sound pressure and field pressure versus tip speed.

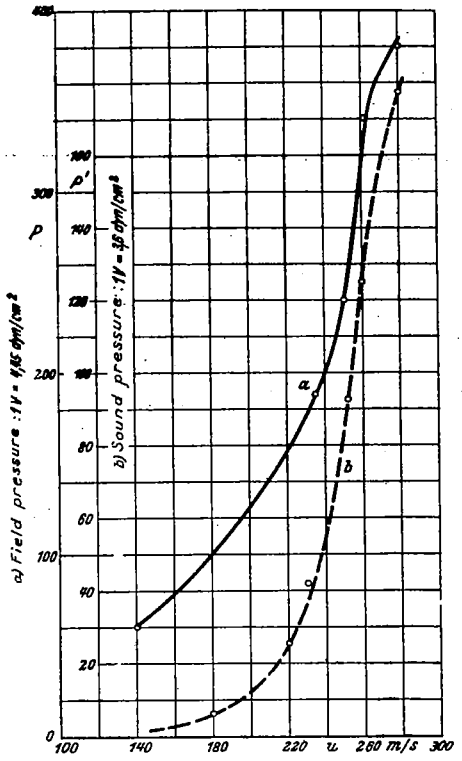

Figure 12.- Sound pressure and field pressure versus tip speed.

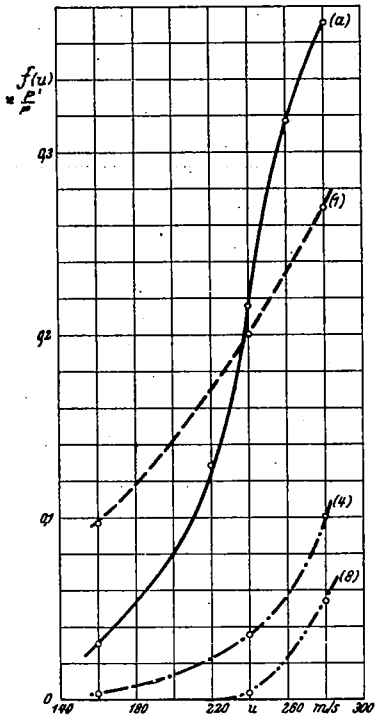

Figure 12a.- Sound pressure and field pressure versus tip speed.

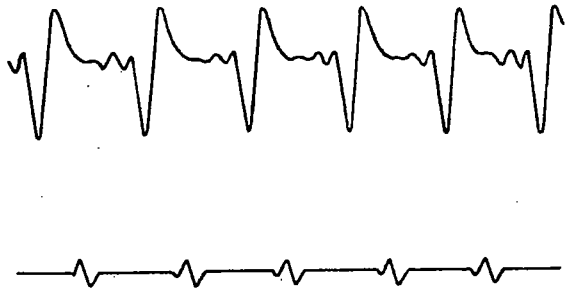

Figure 13.- Oscillogram of sound pressure in plane of propeller.

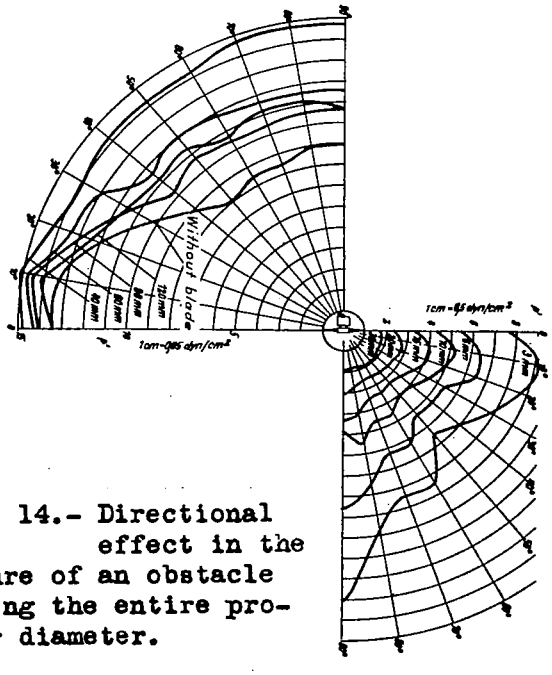

Figure 14.- Directional effect in the pressure of an obstacle spanning the entire propeller diameter.

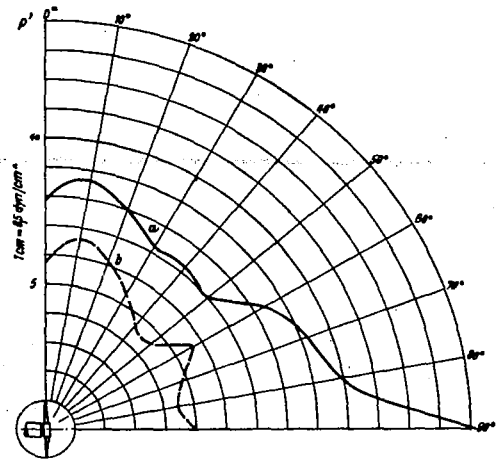

Figure 15.- Directional effect in the presence of an obstacle extending;a) over the entire diameter;b) only over the radius.

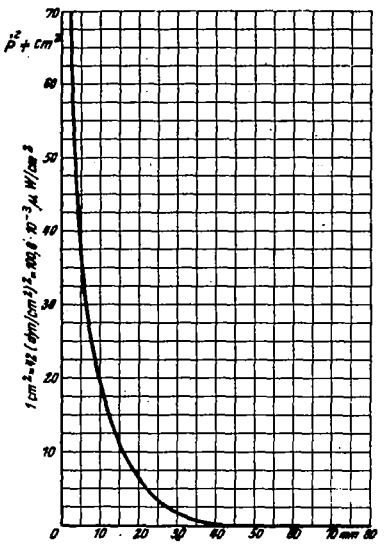

Figure 16.- Sound intensity versus obstacle distance.

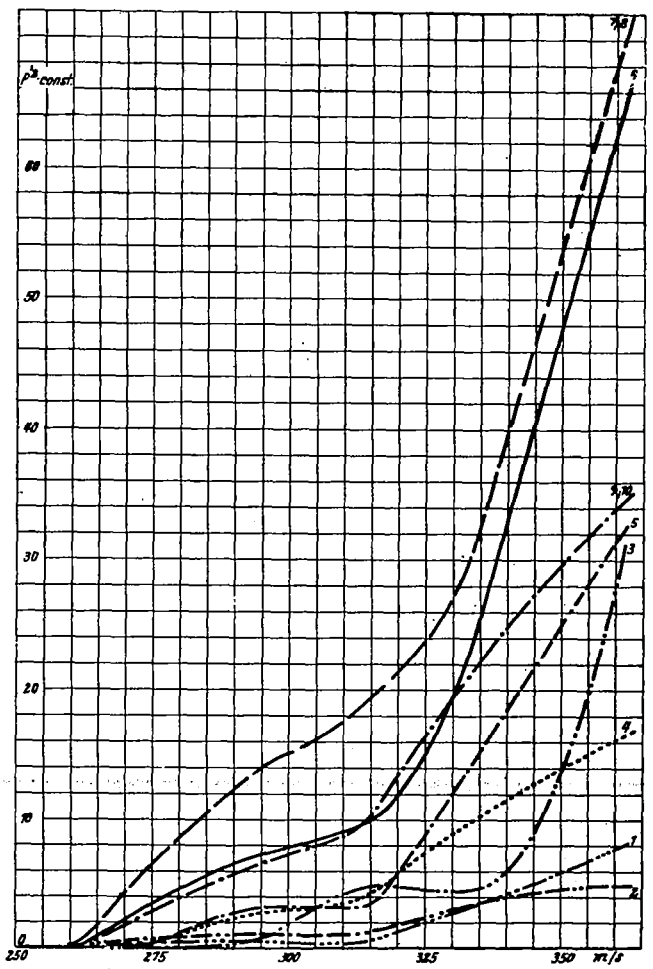

Figure 17.- Sound intensity of the harmonics versus tip speed.

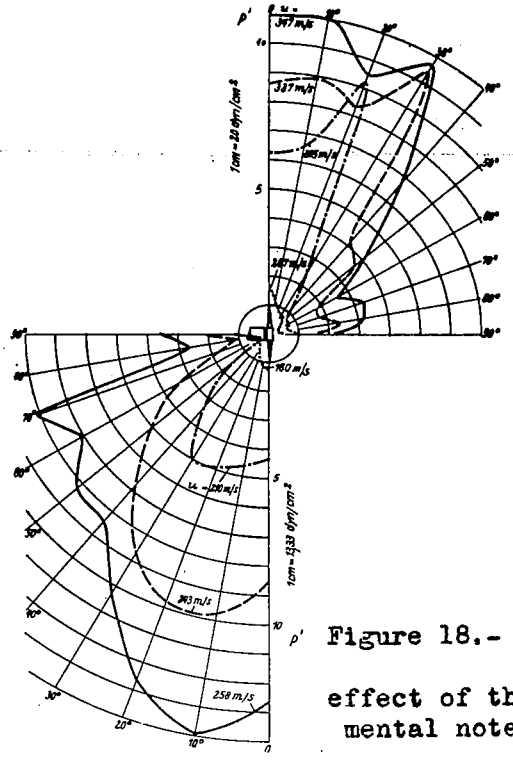

Figure 18.- Directional effect of the fundamental note.

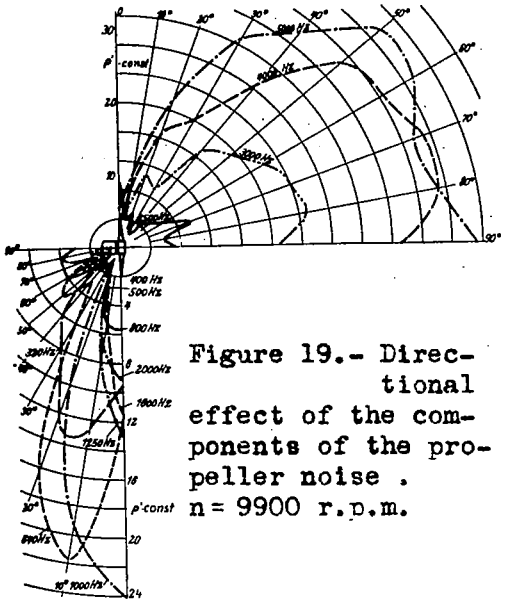

Figure 19.- Directional effect of the components of the propeller noise . n = 9900 r.p.m.

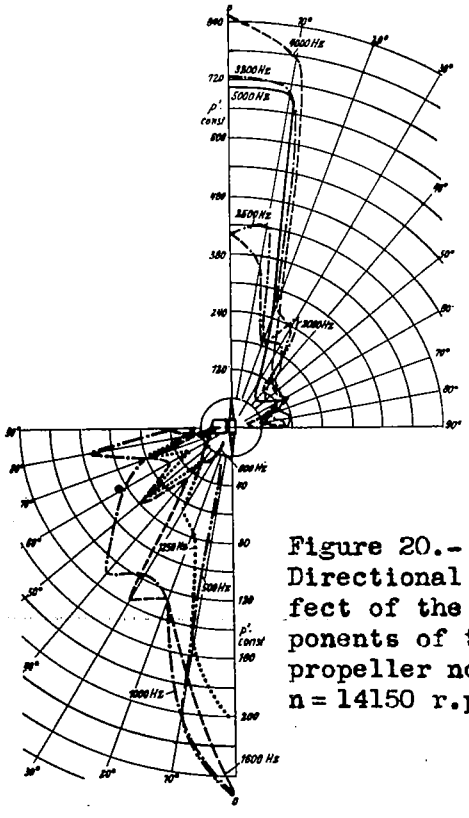

Figure 20.- Directional effect of the components of the propeller noise. n = 14150 r.p.m.

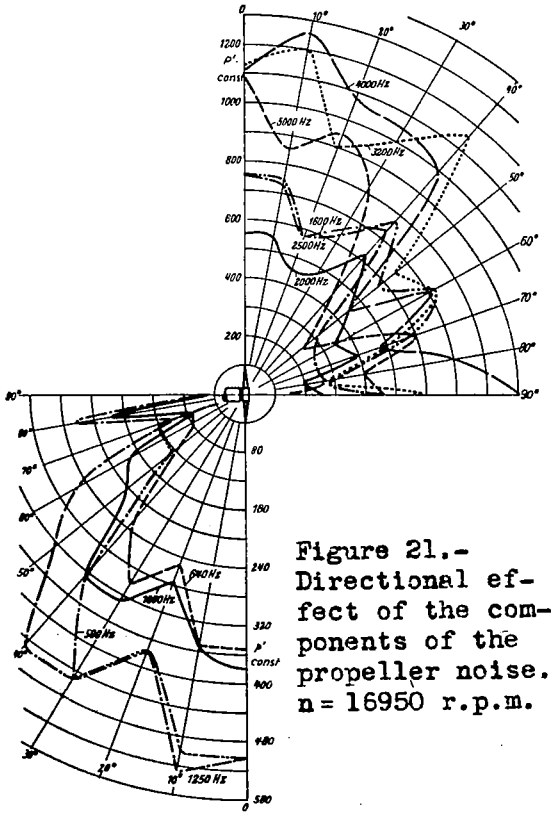

Figure 21.- Directional effect of the components of the propeller noise. n = 16950 r.p.m.

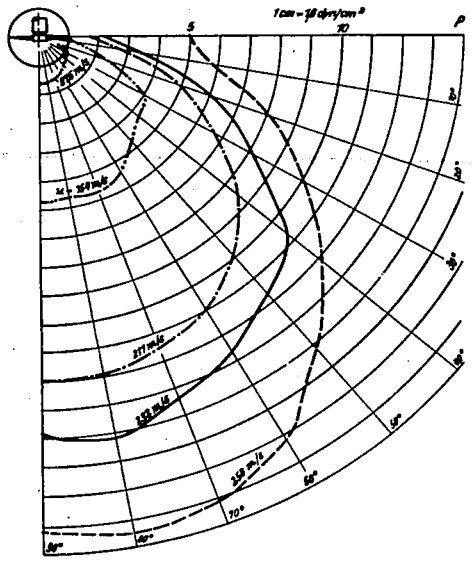

Figure 22.- Directional effect of rotation noise.

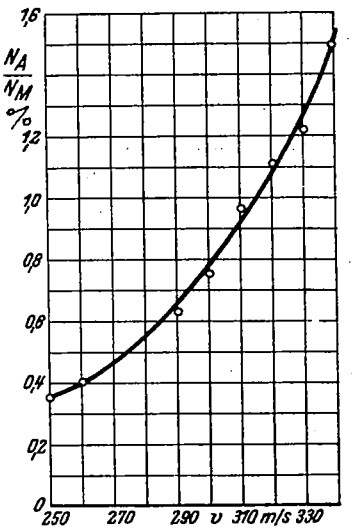

Figure 24.- Ratio of acoustical power to power loss of propeller versus tip speed.

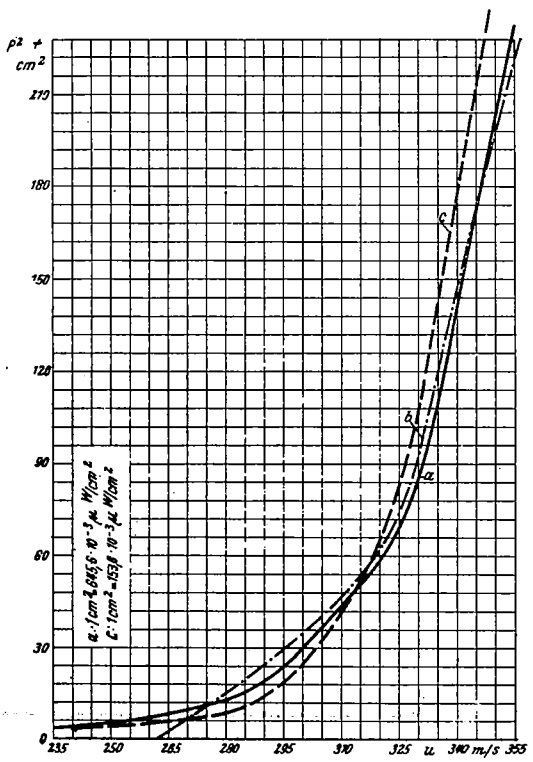

Figure 23.- Sound intensity of rotation note and of rotation noise versus tip speed.